

## Detect 130 Targets

in Single Cells With Pre-Optimized  
Antibody Cocktails Using TotalSeq™-C



BioLegend®

Learn More



The Journal of  
Immunology

This information is current as  
of October 9, 2020.

## Essential Role of NADPH Oxidase– Dependent Production of Reactive Oxygen Species in Maintenance of Sustained B Cell Receptor Signaling and B Cell Proliferation

Yang-Yang Feng, Miao Tang, Mitsuhiro Suzuki, Chinthika  
Gunasekara, Yuki Anbe, Yuichi Hiraoka, Jun Liu, Helmut  
Grasberger, Mamoru Ohkita, Yasuo Matsumura, Ji-Yang  
Wang and Takeshi Tsubata

*J Immunol* published online 13 March 2019  
<http://www.jimmunol.org/content/early/2019/03/13/jimmunol.1800443>

**Supplementary Material** <http://www.jimmunol.org/content/suppl/2019/03/13/jimmunol.1800443.DCSupplemental>

Why *The JI*? [Submit online.](#)

- **Rapid Reviews! 30 days\*** from submission to initial decision
- **No Triage!** Every submission reviewed by practicing scientists
- **Fast Publication!** 4 weeks from acceptance to publication

*\*average*

**Subscription** Information about subscribing to *The Journal of Immunology* is online at:  
<http://jimmunol.org/subscription>

**Permissions** Submit copyright permission requests at:  
<http://www.aai.org/About/Publications/JI/copyright.html>

**Email Alerts** Receive free email-alerts when new articles cite this article. Sign up at:  
<http://jimmunol.org/alerts>

*The Journal of Immunology* is published twice each month by  
The American Association of Immunologists, Inc.,  
1451 Rockville Pike, Suite 650, Rockville, MD 20852  
Copyright © 2019 by The American Association of  
Immunologists, Inc. All rights reserved.  
Print ISSN: 0022-1767 Online ISSN: 1550-6606.



# Essential Role of NADPH Oxidase–Dependent Production of Reactive Oxygen Species in Maintenance of Sustained B Cell Receptor Signaling and B Cell Proliferation

Yang-Yang Feng,\* Miao Tang,\* Mitsuhiro Suzuki,\* Chinthika Gunasekara,\*<sup>1</sup>  
 Yuki Anbe,\* Yuichi Hiraoka,<sup>†,‡</sup> Jun Liu,<sup>§</sup> Helmut Grasberger,<sup>¶</sup> Mamoru Ohkita,<sup>||</sup>  
 Yasuo Matsumura,<sup>||</sup> Ji-Yang Wang,<sup>\*§</sup> and Takeshi Tsubata\*

Reactive oxygen species (ROS) are not only toxic substances inducing oxidative stress but also play a role as a second messenger in signal transduction through various receptors. Previously, B cell activation was shown to involve prolonged ROS production induced by ligation of BCR. However, the mechanisms for ROS production and ROS-mediated activation in B cells are still poorly understood. In this study, we demonstrate that BCR ligation induces biphasic ROS production in both mouse spleen B cells and the mouse B cell line BAL17; transient and modest ROS production is followed by sustained and robust ROS production at 2–6 h after BCR ligation. ROS production in the late phase but not in the early phase augments activation of signaling pathways, such as the NF- $\kappa$ B and PI3K pathways, and is essential for B cell proliferation. ROS production in the late phase appears to be mediated by NADPH oxidases (NOXes) because prolonged ROS production is inhibited by various NOX inhibitors, including the specific inhibitor VAS2870. BCR ligation–induced ROS production is also inhibited by CRISPR/Cas9-mediated deletion of either the *Cyba* gene encoding p22<sup>phox</sup>, the regulator of NOX1–4 required for their activation, or *NOX3*, whereas ROS production is not affected by double deficiency of the *DUOX1* and *DUOX2* genes essential for the activation of the NOX isoforms DUOX1 and DUOX2. These results indicate that NOXes play a crucial role in sustained but not early BCR signaling and suggest an essential role of NOX-dependent sustained BCR signaling in B cell activation. *The Journal of Immunology*, 2019, 202: 000–000.

**B** cell receptor signaling plays a crucial role in B cell responses to Ags, resulting in either the production of specific Abs or B cell tolerance (1). BCR ligation activates protein tyrosine kinases, such as Lyn and Syk, which phosphorylate various signaling molecules, including SLP-65/BLNK, phospholipase C $\gamma$ , and Vav, leading to the activation of transcriptional factors, including NF- $\kappa$ B and NF-AT, and the modulation of cytoskeletons (2–5). BCR signaling is negatively regulated by various phosphatases,

such as Src homology region 2 domain-containing phosphatase-1 (SHP-1), SHIP-1, and PTEN that dephosphorylate signaling molecules activated by BCR ligation (6–9). BCR signaling uses signaling pathways similar to those in TCR signaling. Sustained TCR signaling is required for T cell proliferation and IL-2 secretion (10, 11), and various molecules that are specifically involved in sustained TCR signaling have been identified (12–15). However, roles and molecular mechanisms for sustained BCR signaling are poorly understood.

Reactive oxygen species (ROS), such as superoxide and hydrogen peroxide, are not only toxic substances inducing oxidative stress but also play a role as a second messenger in signal transduction (16–18). Indeed, ROS production is associated with signal transduction through various receptors, including BCR, TCR, TLRs, and cytokine receptors, and signaling through these receptors are downmodulated by treatment with ROS scavengers (17). ROS regulate signaling by reversibly oxidizing various signaling molecules (16, 19, 20). Hydrogen peroxide reversibly oxidizes protein tyrosine phosphatases, such as protein tyrosine phosphatase 1B (PTP1B), SHP-2, and PTEN at the catalytic cysteine residue. Oxidation of these phosphatases inhibits phosphatase activity, thereby augmenting cell signaling. Moreover, ROS regulate various kinases, such as Src family kinases, and transcriptional factors, such as NF- $\kappa$ B and p53, by reversible oxidation. ROS are also known to regulate various other molecules, including calcium channels and inflammasomes.

ROS are produced by various distinct mechanisms in eukaryotes (18, 19, 21). Superoxide anion is produced by mitochondrial respiratory chain and NADPH oxidases (NOXes). Superoxide anion is rapidly converted to hydrogen peroxide by superoxide dismutase (SOD) 1 in cytosol or SOD2 in mitochondrial matrix. Hydrogen peroxide is also produced by other enzymes, such

\*Department of Immunology, Medical Research Institute, Tokyo Medical and Dental University, Tokyo 113-8510, Japan; <sup>†</sup>Department of Molecular Neuroscience, Medical Research Institute, Tokyo Medical and Dental University, Tokyo 113-8510, Japan; <sup>‡</sup>Laboratory of Recombinant Animals, Medical Research Institute, Tokyo Medical and Dental University, Tokyo 113-8510, Japan; <sup>§</sup>School of Basic Medical Sciences, Fudan University, Shanghai 200032, China; <sup>¶</sup>Department of Medicine, University of Michigan, Ann Arbor, MI 48109; and <sup>||</sup>Laboratory of Pathological and Molecular Pharmacology, Osaka University of Pharmaceutical Sciences, Takatsuki, Osaka 569-1094, Japan

<sup>1</sup>Current address: Department of Microbiology, Faculty of Medical Sciences, University of Sri Jayewardenepura, Nugegoda, Sri Lanka.

ORCID: 0000-0002-6003-3088 (C.G.); 0000-0003-0760-1258 (T.T.).

Received for publication March 23, 2018. Accepted for publication February 25, 2019.

This work was supported in part by Japan Society for the Promotion of Science KAKENHI Grants 23390063 and 26293062 (to T.T.).

Address correspondence and reprint requests to Prof. Takeshi Tsubata, Department of Immunology, Medical Research Institute, Tokyo Medical and Dental University, 1-5-45 Yushima, Bunkyo-ku, Tokyo 113-8510, Japan. E-mail address: tsubata.imm@mri.tmd.ac.jp

The online version of this article contains supplemental material.

Abbreviations used in this article: crRNA, CRISPR RNA; DPI, diphenyleneiodonium; IKK, I $\kappa$ B kinase; NAC, *N*-acetylcysteine; NOX, NADPH oxidase; ROS, reactive oxygen species; sgRNA, single guide RNA.

Copyright © 2019 by The American Association of Immunologists, Inc. 0022-1767/19/\$37.50

as xanthine oxidase, cyclooxygenase, and cytochrome p450 mono-oxygenase. These mechanisms, except for NOXes, produce ROS as byproducts of the main enzymatic activities, whereas NOXes are the enzymes whose primary function is regulating ROS production. Among these mechanisms, the mitochondrial respiratory chain and NOXes are the major sources of ROS production. Both ROS production in mitochondria and that by NOXes are known to play a role in signaling through various receptors, including TLRs, NLRP3 inflammasomes, TCR, BCR, and cytokine receptors (17). In T cells, the inhibition of mitochondrial ROS production by knockout or knockdown of the components of mitochondrial respiratory chains inhibits expression of IL-2 and IL-4 induced by TCR ligation and T cell proliferation (22, 23). Enhanced ROS production in mitochondria enhances RIG-I-like receptor and TLR signaling (24, 25). In contrast, knockout or knockdown of NOXes inhibits NLRP3 inflammasome activation induced by silica and asbestos (26) and cytokine signaling through IL-1R, platelet-derived growth factor receptor (PDGFR), and TNFR (27–29).

NOXes are the family of transmembrane enzymes that generate superoxide from NADPH and oxygen (21, 30). There are seven isoforms of NOX1-5, DUOX1, and DUOX2. However, rodents lack NOX5. Most of these isoforms require association with interaction partners for the catalytic activity. NOX1-4 associate with the small membrane protein p22<sup>phox</sup>, whereas DUOX1 and DUOX2 associate with DUOXA1 and DUOXA2, respectively. These associations are required for the oxidase activity. Activation of NOX1, 2, and 3 also requires stimulation-dependent association with distinct cytosolic proteins for each isoform p47<sup>phox</sup>, p67<sup>phox</sup>, and p40<sup>phox</sup> for NOX2 and NOX1 and NOXA1 for NOX1 and NOX3. NOX4 does not require association with cytosolic proteins for activation and is thus thought to be constitutively active.

A potential role of ROS in BCR signaling was first suggested by the observation that treatment of B cells with H<sub>2</sub>O<sub>2</sub> induces signaling through BCR in the absence of BCR ligation (31). Studies using NOX2<sup>-/-</sup> mice demonstrated that superoxide is produced within a few minutes after BCR is ligated dependently on NOX2 (32). However, NOX2<sup>-/-</sup> B cells showed normal early BCR signaling, including Ca<sup>2+</sup> mobilization, the phosphorylation of various signaling molecules, such as AKT and Syk, and BCR ligation-induced B cell proliferation (32). This study clearly demonstrated that ROS are not involved in early BCR signaling, although other studies suggested the involvement of ROS in BCR signaling through the inhibition of protein tyrosine phosphatases (PTPs) (33, 34). In contrast, Wheeler and DeFranco demonstrated that BCR ligation induces prolonged but not immediate ROS production in NOX2<sup>-/-</sup> B cells, and the scavenging of ROS inhibited proliferation of these B cells (35). Thus, prolonged ROS production after BCR ligation plays a crucial role in B cell activation. These authors suggested that prolonged ROS production involves mitochondria but not NOXes because they detected ROS production using an ROS indicator targeted to mitochondria but failed to detect expression of NOXes other than NOX2 (35). In this study, we analyze the expression of NOXes in mouse B cell lines and normal mouse spleen B cells and detect the expression of NOX1, NOX2, NOX3, DUOX2, and their regulators. BCR ligation-induced sustained ROS production is almost completely inhibited by specific NOX inhibitors and the deletion of the *Cyba* gene encoding p22<sup>phox</sup> required for NOX-induced ROS production. Deletion of NOX3 but not NOX1 also reduces BCR ligation-induced sustained ROS production. Moreover, we demonstrate that sustained ROS production enhances the sustained activation of NF-κB and PI3K pathways. Our results strongly suggest the involvement of NOXes in BCR ligation-induced prolonged ROS production required for sustained BCR signaling and B cell proliferation.

## Materials and Methods

### Mice

C57BL/6 (B6) mice were purchased from Sankyo Laboratory Service (Tokyo, Japan). NOX2<sup>-/-</sup> mice (36) and mice deficient in both DUOXA1 and DUOXA2 (DUOXA<sup>-/-</sup> mice) (37) were described previously. Mice were bred and maintained in the animal facility of Tokyo Medical and Dental University under specific pathogen-free conditions. Because DUOXA<sup>-/-</sup> mice develop severe hypothyroidism, DUOXA<sup>-/-</sup> mice were s.c. injected daily with 40 ng/g body weight L-thyroxine (Wako Chemicals) after P6 or fed with drinking water containing 0.26 mg/l L-thyroxine after weaning. All animal experiments were approved by the Institutional Animal Care and Use Committee of Tokyo Medical and Dental University and were performed according to our institutional guidelines.

### Cells

Mouse spleen B cells were isolated as described previously (38). Spleen B cells and the mouse B cell line BAL17 were cultured in RPMI 1640 medium supplemented with 10% FCS, 50 μM 2-ME, 1 mM L-glutamine, and 100 U/ml penicillin/streptomycin (complete RPMI 1640 medium) in the presence or absence of 10 μg/ml F(ab')<sub>2</sub> fragments goat anti-mouse IgM Ab (Jackson ImmunoResearch Laboratories), 10 mM N-acetylcysteine (NAC) (Sigma-Aldrich), 1.25 or 2.5 μM VAS2870 (Calbiochem), 100 μM apocynin (Cayman Chemical), 5 μM diphenyleneiodonium (DPI) (Sigma-Aldrich), 2 μg/ml antimycin A (Sigma-Aldrich), 1 or 10 μg/ml anti-mouse CD40 Ab FGK45 (39), or 20 ng/ml IL-4 (PeproTech). HEK 293T cells and the retrovirus packaging cell line PLAT-E (a gift of Dr. T. Kitamura, University of Tokyo, Tokyo, Japan) (40) were maintained in DMEM supplemented with 10% FCS, 2 mM L-glutamine, and 100 U/ml penicillin/streptomycin.

### Measurement of intracellular ROS production

After incubation with anti-IgM Ab (Jackson ImmunoResearch Laboratories), B cells were incubated with 2 μM ROS-sensitive probe 5-(and-6)-chloromethyl-2',7'-dichlorodihydrofluorescein diacetate (Invitrogen) in Hybridoma-SFM (Invitrogen) at 37°C for 10 min. For detection of ROS in mitochondria, B cells were loaded with 5 μM MitoSOX Red (Invitrogen) in RPMI 1640 containing 10% FCS at 37°C for 20 min before incubation with anti-IgM. In some samples, cells were treated with 2 μg/ml antimycin A (Sigma-Aldrich) for the last 1 h of incubation. Cells were analyzed by flow cytometry using FACSVerse.

### CFSE assay for cell proliferation

Cells were stained with 2 μM CFSE (Invitrogen) in serum-free RPMI 1640 medium at 37°C for 10 min. Staining was terminated by the addition of equal volume ice-cold RPMI 1640 containing 10% FCS and incubated on ice for 5 min. Cells were cultured in a total volume of 200 μl complete RPMI 1640 medium at 37°C for 72 h. The reduction of the CFSE fluorescence at each cell division was analyzed by flow cytometry using FACSVerse to determine the number of cell divisions.

### Flow cytometry

Cells were incubated with anti-FcγRII/III Ab 2.4G2 for 10 min to block FcγRII/III-mediated binding and were stained for 30 min on ice with the following Abs: Pacific Blue- or Alexa Fluor 647-conjugated anti-mouse B220 (RA3-6B2), biotin-conjugated anti-mouse CD19 (eBioscience), Alexa Fluor 488-conjugated streptavidin (Invitrogen), Pacific Blue-conjugated anti-mouse IgM, FITC-conjugated anti-mouse IgM (SouthernBiotech), PE-conjugated anti-mouse CD5 (BioLegend), FITC-conjugated anti-mouse CD21 (BioLegend), PE-conjugated anti-mouse CD23 (eBioscience), Alexa Fluor 647-conjugated anti-mouse IgD (BioLegend), and PE-conjugated anti-mouse CD138 (BD Pharmingen). For detecting dead cells, cells were stained with propidium iodide (Nacalai Tesque).

### ELISA

The concentration of IgG was measured by standard sandwich ELISA using unlabeled and alkaline phosphatase-conjugated goat anti-mouse IgG (SouthernBiotech).

### RT-PCR

Colon, testis, kidney, and thyroid gland were isolated from C57BL/6 mice and homogenized. Total RNA was extracted from spleen B cells, BAL17 cells, colon, testis, kidney, and thyroid gland by TRIzol (Invitrogen). cDNA was synthesized using SuperScript III Reverse Transcriptase (Invitrogen) according to the manufacturer's instructions. DNA fragments encoding

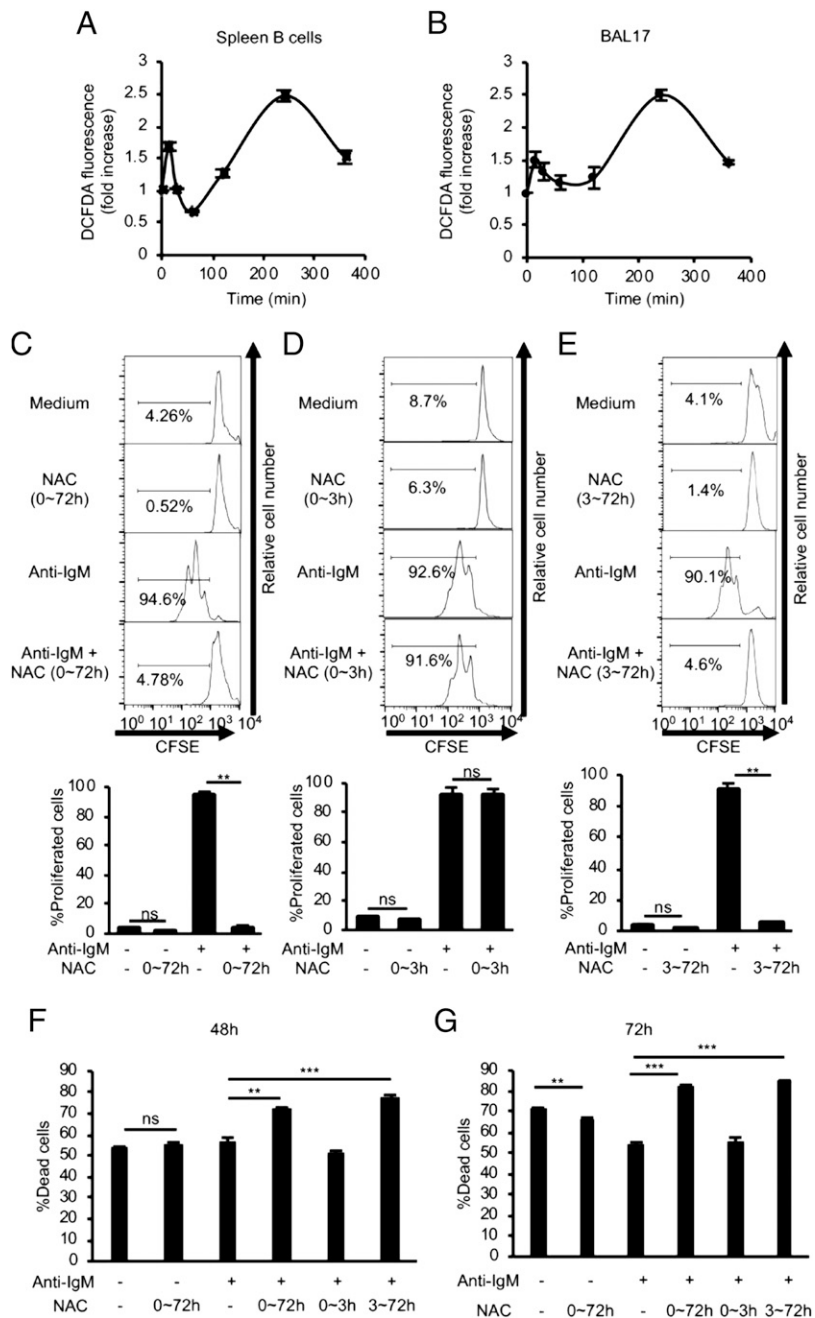


**FIGURE 1.** BCR ligation-induced prolonged ROS production is crucial for B cell proliferation. (**A** and **B**) BCR ligation induces ROS production in two phases. Spleen B cells from wild-type C57BL/6 mice (**A**) and BAL17 cells (**B**) were stimulated with 10  $\mu\text{g/ml}$  anti-IgM Ab for different times. Cells were loaded with the ROS indicator DCFDA, and DCFDA fluorescence was measured by flow cytometry. Fold changes in mean fluorescence intensity of DCFDA fluorescence compared with untreated cells were calculated. (**C–E**) ROS production in the late phase is required for BCR ligation-induced B cell proliferation. Spleen B cells from C57BL/6 mice were loaded with CFSE and stimulated with anti-IgM for 72 h in the presence or absence of 10 mM NAC either at 0–72 h (**C**), 0–3 h (**D**), or 3–72 h (**E**). CFSE fluorescence was measured by flow cytometry (upper panels). Percentages of proliferated cells are indicated. Mean  $\pm$  SD of triplicate is shown.  $**p < 0.01$ , ns; not significant (Student *t* test). Data represent three independent experiments. (**F** and **G**) ROS production in the late phase enhances B cell survival. Spleen B cells from C57BL/6 mice were stimulated with anti-IgM for 48 h (**F**) or 72 h (**G**) in the presence or absence of 10 mM NAC at indicated times. Percentages of dead cells were determined by flow cytometry using propidium iodide. Mean  $\pm$  SD of triplicate is shown.  $**p < 0.01$ ,  $***p < 0.001$ ; ns, not significant (Dunnett test).

various Nox isoforms and their regulators were amplified by PCR using specific primers. PCR amplification conditions were 94°C for 3 min; 35 cycles of 94°C for 30 s, 55°C for 30 s, and 72°C for 30 s; and 72°C for 5 min. PCR products were analyzed by 1.5% agarose gel electrophoresis. The *Cyba* cDNA was amplified from cDNA of BAL17 cells using forward (5'-TACGAATTCCACCATGGGGCAGATCGAGTGGG-3') and reverse (5'-TCCGGAATTCTCACACGACCTCATCTGTCAC-3') primers.

#### Generation of *Cyba*<sup>-/-</sup>, *Nox1*<sup>-/-</sup>, and *Nox3*<sup>-/-</sup> BAL17 cells using a CRISPR/Cas9 system

The single guide RNA (sgRNA) sequences targeting exon 3 in the *Cyba* gene (5'-TGTCTGCTGGAGTATCCCCG-3') and exon 1 in the *Nox3* gene (5'-TCGTTCCAGAATCCAGCACAC-3') were designed using online software provided by Benchling (<https://benchling.com/>). The sgRNA sequence targeting exon 10 in the *Nox1* gene (5'-TGAGCTTGTGTGCGGCACGC-3') was designed using online CRISPRscan predictions (<http://crisprscan.org/>). The oligonucleotides encoding sgRNAs were annealed with complementary oligonucleotides and then ligated into the BsmBI (R0580; New England BioLabs)-digested lentiCRISPR vector (49535; Addgene) (41–43). Lentivirus was produced by the triple transfection of HEK-293T cells with the

lentiCRISPR vector encoding sgRNAs, together with the packaging plasmid psPAX2 (Addgene) and pMD2.G encoding VSV-G envelope (Addgene) using polyethylenimine (PolyScience) in DMEM containing 10% FCS. After 72 h, virus-containing supernatant was collected, and BAL17 cells were infected by spin infection in the presence of 10  $\mu\text{g/ml}$  hexadimethrine bromide (polybrene) (Nacalai Tesque). After the addition of equal volume of complete RPMI medium, cells were cultured for 24 h in complete RPMI and then selected in the presence of 0.25  $\mu\text{g/ml}$  puromycin (Wako Chemicals) for 5 d. Puromycin-resistant cells were cloned by limiting dilution. Wells containing a single colony were selected under a microscope and expanded. Genomic DNA was extracted, and the targeted sequences were amplified by PCR and sequenced.

#### Restoration of *Cyba* expression

*Cyba* cDNA amplified by RT-PCR was cloned in the pMD20-T vector using Mighty TA-cloning Kit (Takara Bio). Eight nucleotides substitutions were introduced into the sgRNA-targeting site of the *Cyba* cDNA without altering the amino acid sequence of the protein by PCR using forward (5'-GCTTACTCGAATACCCTAGGGGAAAGAGGAAAAGGGGTC-3') and reverse (5'-CTAGGGTATTTCGAGTAAGCAGATGAGCACACCTGCAGC-3')

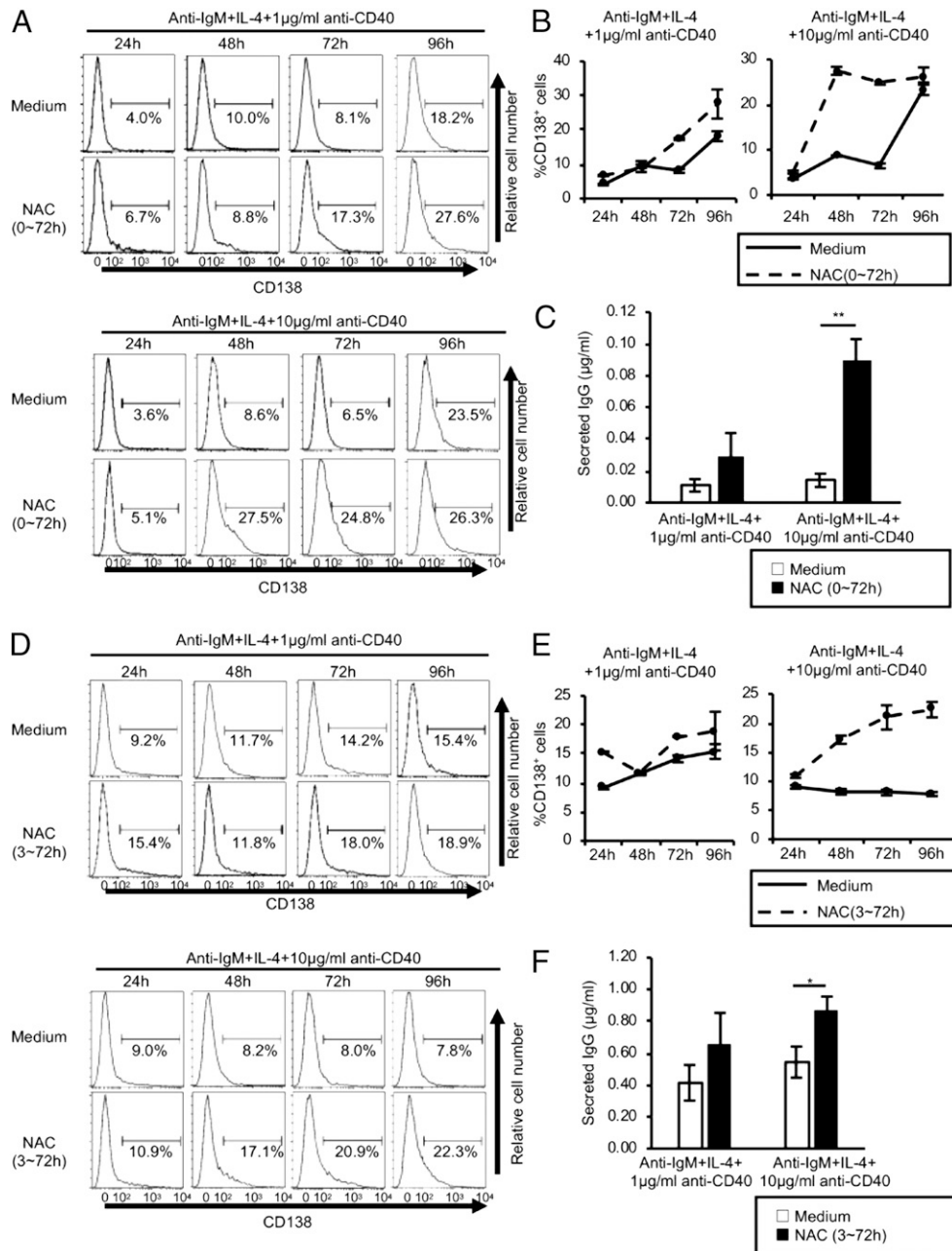


**FIGURE 2.** BCR ligation-induced prolonged ROS production delays B cell differentiation to plasma cells. Spleen B cells from C57BL/6 mice were cultured with anti-IgM, IL-4, and 1 or 10 μg/ml anti-CD40 Ab for indicated times. NAC was added to the culture at the beginning (A–C) or at 3 h of culture (D–F). Expression of CD138 was analyzed by flow cytometry (A and D). Percentages of CD138<sup>+</sup> cells were calculated and mean ± SD of triplicate is shown (B and E). Concentrations of IgG in the culture supernatants at 96 h were measured by ELISA (C and F). Mean ± SD of triplicate is shown. \**p* < 0.05, \*\**p* < 0.01 (Student *t* test).

primers. The DNA fragment containing the mutated *Cyba* cDNA was isolated from the T vector using EcoRI and ligated into the EcoRI-digested pMXs-ires-iRFP720 vector (pMXs-Cybamut-ires-iRFP720), which was generated by replacing the NcoI-SalI fragment encoding GFP in pMXs-ires-GFP (a gift of Dr. Kitamura) (44) with the NcoI-SalI fragment containing iRFP720 isolated from piRFP720-N1 (Addgene). Retrovirus was produced by transfection of PLAT-E cells with pMXs-Cybamut-ires-iRFP720 using polyethylenimine reagent, and *Cyba*<sup>-/-</sup> BAL17 cells were infected. Red fluorescence protein-positive cells were sorted using MoFlo XDP (Beckman Coulter).

#### Generation of *Cyba*<sup>-/-</sup> mice

CRISPR/Cas9-mediated genome editing was done by using cloning-free CRISPR/Cas system as described previously (45). For deleting the *Cyba* exons 1–3, CRISPR RNAs (crRNAs) were designed in exon 1 (5'-UGU-CUGCUGGAGUAUCCCGGUUUUAGAGCUAUGCUGUUUUU-3')

exon 3 (5'-ACUCGAUCUGCCCCAUGACGGUUUUAGAGCUAUGCU-UUUUUU-3'). A single-stranded oligo DNA donor, which contains 75 bp up- or downstream region from DNA double-strand breaking sites determined by each crRNAs, were coinjected to a fertilized egg with all the CRISPR/Cas9 components including crRNAs and a *trans*-activating crRNA. All the oligonucleotides were chemically synthesized and purified by high-pressure liquid chromatography (FASMAC, Atsugi, Japan).

#### Western blotting

Total cell lysates were separated by SDS-PAGE and blotted to PVDF membranes (Immobilon). Membranes were reacted by mouse anti-IκBα mAb (L35A5), rabbit anti-phospho-IκBα mAb (Ser32) (14D4), mouse anti-IκB kinase (IKK) β mAb (3G12), rabbit anti-IKKβ mAb (D30C6), rabbit anti-phospho-IKKα/β mAb (Ser176/180) (16A6), rabbit anti-NF-κB p65 mAb (D14E12), rabbit anti-phospho-NF-κB p65 mAb (Ser536) (93H1), rabbit anti-CARD11 mAb (1D12), rabbit anti-phospho-CARD11

mAb, rabbit anti-phospho-Akt mAb (Ser473) (all from Cell Signaling Technology), anti- $\beta$  tubulin (TUB 2.1) (Santa Cruz Biotechnology), rabbit anti-mouse p22<sup>phox</sup> Ab (Bioworld), rabbit anti-Nox1 Ab (GeneTex) or rabbit anti-Nox3 Ab (Abclonal Technology), mouse anti-mouse NOXO1 Ab (Santa Cruz Biotechnology), rabbit anti-mouse NOXA1 Ab (Bioss Antibodies), and rabbit anti-mouse DUOX2 Ab (Abcam), followed by a reaction with HRP-conjugated anti-rabbit IgG Ab (Invitrogen) or HRP-conjugated anti-mouse IgG Ab (Cell Signaling Technology). Proteins were then visualized using enhanced Chemi-Lumi One L (Nacalai Tesque).

### Statistics

Data were analyzed by unpaired Student *t* test or Dunnett test.

## Results

### Prolonged ROS production after BCR ligation is required for B cell proliferation

To address the time course of ROS production after BCR ligation, we ligated BCR with anti-IgM Ab and measured the ROS level using ROS-sensitive dye DCFDA in both mouse spleen B cells and BAL17 cells at various time points. In spleen B cells, the ROS level was increased at 15 min after BCR ligation and returned to the basal level in 1 h (Fig. 1A, Supplemental Fig. 1A, 1C). The ROS level was again increased after 1 h and reached the second peak at 4 h after BCR ligation. The ROS level in the second phase is much higher than that in the first phase. Essentially, the same result was obtained in BAL17 cells (Fig. 1B, Supplemental Fig. 1B, 1D). This result indicates that BCR ligation induces ROS production in two phases: transient ROS production in the early phase within 1 h is followed by stronger and more sustained ROS production at 2–6 h after BCR ligation.

To address the role of ROS production in B cell activation, we examined B cell proliferation by stimulating CFSE-labeled spleen B cells with anti-IgM in the presence or absence of the ROS scavenger NAC. Treatment with NAC completely inhibited B cell proliferation induced by anti-IgM Ab (Fig. 1C). To address the role of ROS production at the early phase and that at the late phase separately, we stimulated B cells with anti-IgM in the presence of NAC either during the first 3 h alone or after 3 h. Although treatment with NAC during the first 3 h did not inhibit B cell

proliferation at all (Fig. 1D), B cell proliferation was completely inhibited by treatment with NAC after 3 h (Fig. 1E). Treatment of NAC increased the percentage of dead cells in anti-IgM-treated spleen B cells, indicating that ROS enhances the survival of BCR-ligated B cells (Fig. 1F, 1G). Moreover, death of anti-IgM-stimulated B cells was augmented by the treatment of NAC after 3 h but not the treatment with NAC during the first 3 h, suggesting that prolonged ROS production enhances the survival of BCR-ligated B cells. Taken together, ROS production at the late phase after 3 h is crucial for both the proliferation and the survival of BCR-ligated B cells.

To address whether ROS regulate B cell differentiation to plasma cells, we stimulated B cells with anti-IgM, anti-CD40, and IL-4 in the presence or absence of NAC. NAC accelerated the generation of CD138<sup>+</sup> cells (Fig. 2A, 2B) and augmented secretion of IgG (Fig. 2C), suggesting that ROS inhibit differentiation to plasma cells (Fig. 2A, 2B). To address the role of ROS production at the late phase in the regulation of plasma cell differentiation, we treated B cells with NAC after 3 h. This treatment accelerates the generation of CD138<sup>+</sup> cells and augments secretion of IgG from spleen B cells (Fig. 2D–F) as efficiently as the treatment with NAC from the beginning of culture does. Thus, prolonged ROS production delays B cell differentiation to plasma cells.

### Prolonged ROS production after BCR ligation involves NOXes but not mitochondrial respiration

To address the mechanisms for ROS production at the late phase in BCR-ligated B cells, we first measured ROS production in mitochondria using mitochondria-targeted ROS-sensitive fluorogenic dye MitoSOX. Although treatment with mitochondrial respiratory chain inhibitor antimycin A for 1 h increases the ROS level in mitochondria in both spleen B cells and BAL17, BCR ligation for 4 h did not increase the mitochondrial ROS level in either spleen B cells or BAL17 (Fig. 3). Thus, mitochondrial respiration is not involved in prolonged ROS production induced by BCR ligation.

Next, we addressed the involvement of NOXes in BCR ligation-induced prolonged ROS production. When we stimulated spleen B cells with anti-IgM in the presence of the NOX inhibitors apocynin or DPI, ROS production at 4 h is almost completely abolished

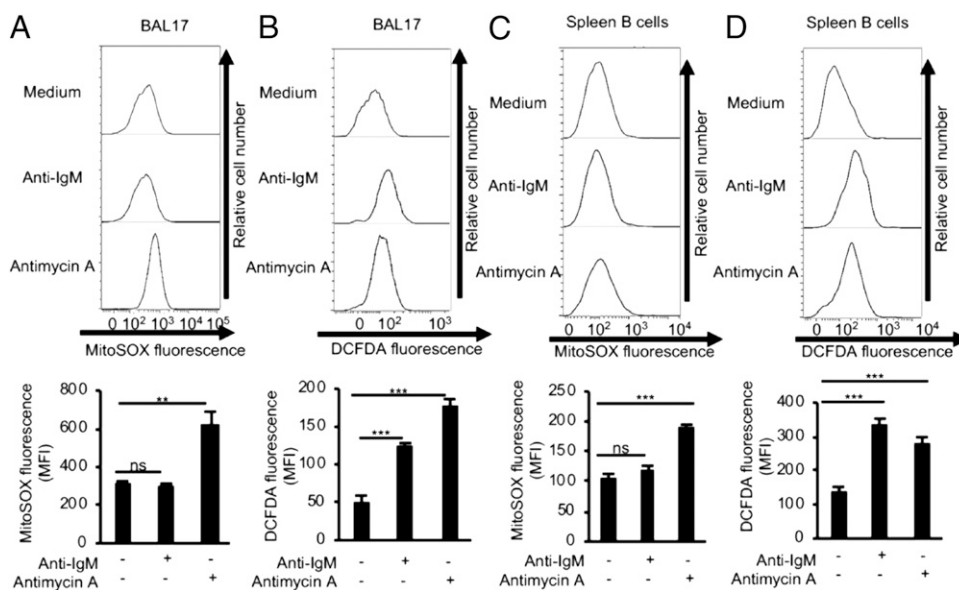


**FIGURE 3.** Mitochondria are not involved in BCR ligation-induced prolonged ROS production. BAL17 cells (A and B) and spleen B cells (C and D) were stimulated with 10  $\mu$ g/ml anti-IgM Ab for 4 h or 2  $\mu$ g/ml antimycin A for 1 h. MitoSOX (A and C) and DCFDA (B and D) were loaded to the cells before or after stimulation, respectively. Fluorescence of MitoSOX and DCFDA is measured by flow cytometry (upper panels), and fold changes in mean fluorescence intensity (MFI) compared with untreated cells were calculated (lower panels). Mean  $\pm$  SD of triplicate is shown. Data represent three independent experiments. \*\**p* < 0.01, \*\*\**p* < 0.001; ns, not significant (Dunnett test).

**FIGURE 4.** BCR ligation-induced prolonged ROS production and B cell proliferation are abrogated by NOX inhibitors. Spleen B cells from C57BL/6 mice were loaded with CFSE (B, D, and E). CFSE-loaded or unloaded cells (A and C) were stimulated with 10  $\mu$ g/ml anti-IgM (A–D) or 1  $\mu$ g/ml LPS (E) in the presence of apocynin (A and B), DPI (A), or VAS2870 (VAS) (C–E) for 4 h (A), 72 h (B, D, and E), or indicated times (C). Cells were loaded with DCFDA in the presence or absence of DPI (A), apocynin (A), or VAS2870 (VAS) (C). Fluorescence of DCFDA (A and C) or CFSE (B, D, and E) were measured by flow cytometry. Fold changes in mean fluorescence intensity (MFI) of DCFDA fluorescence compared with untreated cells were calculated (A and C). Alternatively, percentages of proliferated cells are indicated (B, D, and E). Mean  $\pm$  SD of triplicate is shown (A and lower panels of B, D, and E). Data were analyzed by Student *t* test (A) or Dunnett test (B, D, and E). \*\**p* < 0.01, \*\*\**p* < 0.001; ns, not significant.

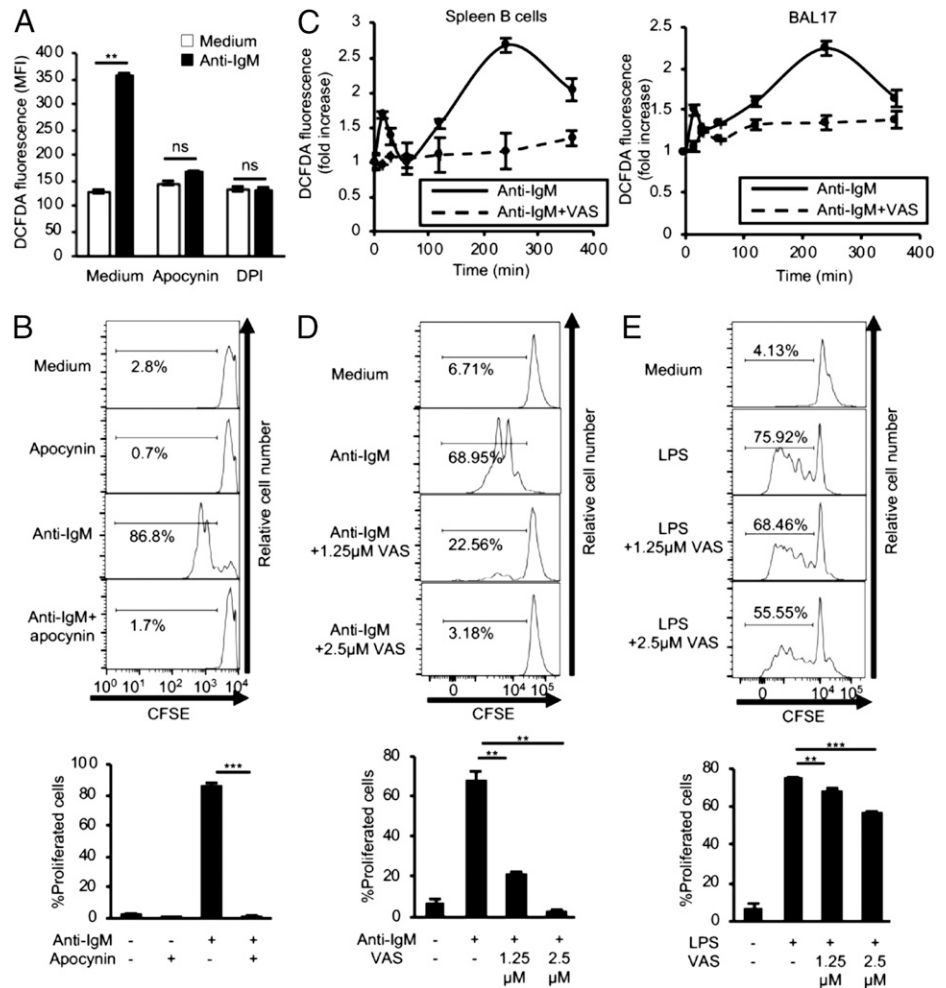


(Fig. 4A). Apocynin also completely abolished the proliferation of B cells stimulated with anti-IgM (Fig. 4B). These results suggest that NOXes are required for prolonged ROS production and the proliferation of B cells induced by BCR ligation. However, classical NOX inhibitors were not specific to NOXes. DPI inhibits enzymes involved in mitochondrial respiration, and apocynin carries ROS-scavenging activity in addition to NOX inhibition (46). To exclude the possibility that these NOX inhibitors reduced the ROS level by scavenging ROS or inhibiting mitochondrial respiration, we used the NOX inhibitor VAS2870, which was shown not to carry an ROS-scavenging activity (47). VAS2870 almost completely inhibited ROS production in both the early and late phases after stimulation with anti-IgM in spleen B cells and BAL17 (Fig. 4C). Moreover, VAS2870 almost completely inhibited the proliferation of spleen B cells stimulated by anti-IgM (Fig. 4D), whereas LPS-induced proliferation was inhibited

by VAS2870 only marginally (Fig. 4E). These results suggest that BCR ligation-induced prolonged ROS production involves NOXes but not mitochondrial respiration.

*B cells express various NOXes and their regulators but do not require NOX2 or DUOX2 for BCR ligation-induced prolonged ROS production*

To address how NOXes are involved in ROS production in B cells after BCR ligation, we examined the expression of various members of NOXes in spleen B cells and BAL17 cells except for NOX2 because it is already established that NOX2 is activated upon BCR ligation (35). We used tissues known to highly express each NOX isoform as controls. By RT-PCR analysis using specific primers (Table I), the expression of NOX1, NOX3, and DUOX2 was readily detected in both BAL17 and spleen B cells, whereas NOX4 and DUOX1 were not detectable in either BAL17 or

Table I. PCR primers

Gene	Forward Primer	Reverse Primer
NOX1	5'-GGTGGGGCTGAACATTTTTTC-3'	5'-TCGACACACAGGAATCAGGAT-3'
NOX3	5'-TGGCAGTAAACGCCTATCTGT-3'	5'-CGGAACCCAGATAACTCGTGT-3'
NOX4	5'-GAAGGGGTAAACACCTCTGC-3'	5'-ATGCTCTGCTTAAACACAATCCT-3'
DUOX1	5'-AAAACACCAGGAACGGATTGT-3'	5'-AGAAGACATTGGGCTGTAGGG-3'
DUOX2	5'-GGCCACAAGGGGTGTATGC-3'	5'-GGCAGCCATTGGTATAGAGCA-3'
NOXA1	5'-AGTGCAGAAACAGGTACCCC-3'	5'-TGCTCAGGACCTCTTACACAT-3'
NOXO1	5'-GAGCCCTTATCCCAACCAG-3'	5'-CAGAAGTGCCTCCCACTTCC-3'
DUOXA1	5'-ACCAAGCCAACCTTTCCAATG-3'	5'-GCCCGATGAATAAGCTGGTC-3'
DUOXA2	5'-GACGGGTGCTACCCCTTTTAC-3'	5'-GCTAAGAAGGACTCTCACCAAC-3'

spleen B cells (Fig. 5A). We next examined the expression of the regulators required for the activity of these NOXes. BAL17 and spleen B cells expressed NOXA1 and NOXO1 required for the activation of NOX1 and NOX3 and DUOX2 (Fig. 5A), which is the transmembrane regulator for DUOX2, whereas DUOX1, which is required for the activation of DUOX1, was not detected in either spleen B cells or BAL17 cells. Western blot analysis showed that NOX1, NOX3, DUOX2, NOXA1, and NOXO1 are expressed at the protein level (Fig. 5B). Because NOX2 is functional in B cells (32, 35), B cells appear to express p22<sup>phox</sup>, which is required for the activity of NOX1-4. These results suggest that NOX1, NOX3, and DUOX2 as well as NOX2 are functional in B cells.

We next addressed whether NOX2, DUOX1, and DUOX2 are involved in BCR ligation-induced ROS production. In spleen B cells from *NOX2*<sup>-/-</sup> mice, BCR ligation-induced ROS production in the early phase was completely abolished, whereas ROS production in the late phase was normal (Fig. 5C, left panel), in agreement with previous findings. ROS production in the late phase was not reduced in spleen B cells from mice deficient in NOX2 and DUOX1/2 (Fig. 5C, right panel), indicating that both DUOX1 and DUOX2 are dispensable in BCR ligation-induced ROS production at the late phase. Moreover, both *NOX2*<sup>-/-</sup> and *NOX2*<sup>-/-</sup> *DUOX1*<sup>-/-</sup> B cells showed BCR ligation-induced proliferation as efficiently as wild-type B cells (Fig. 5D). These results clearly indicate that NOX2, DUOX1, and DUOX2 are not required for either BCR ligation-induced prolonged ROS production or B cell proliferation. Thus, NOX1, NOX3, or both appear to be involved in the prolonged ROS production after BCR ligation because NOX4 expression is not detectable in B cells.

#### The NOX regulator p22<sup>phox</sup> and NOX3, but not NOX1, are essential for BCR ligation-induced prolonged ROS production in the B cell line BAL17

We further addressed whether NOXes are involved in prolonged ROS production after BCR ligation using BAL17 because BAL17 cells show BCR ligation-induced prolonged ROS production sensitive to VAS2870 without generating ROS in mitochondria, which is the case for spleen B cells. We addressed the involvement of NOXes by deleting the *Cyba* gene encoding p22<sup>phox</sup> using a CRISPR/Cas9 system. We expressed CRISPR/Cas9 together with a guide RNA complementary to the target sequence in exon 3 of the *Cyba* gene encoding p22<sup>phox</sup> in BAL17 cells using a lentiviral vector (Fig. 6A). By sequencing exon 3 of the *Cyba* gene in each independent clone, we obtained nine clones that appear to carry mutations in both alleles of *Cyba*. Western blotting revealed that, among nine clones, p22<sup>phox</sup> was not detectable in five clones (Fig. 6B). When we stimulated these *Cyba*<sup>-/-</sup> BAL17 clones with anti-IgM, ROS production at 4 h was either markedly reduced or undetectable (Fig. 6C, 6D), suggesting that p22<sup>phox</sup> is essential for BCR ligation-induced prolonged ROS production.

To exclude off-target effects of CRISPR/Cas9, we chose *Cyba*<sup>-/-</sup> BAL17 clones that show no BCR ligation-induced prolonged ROS production (clones no. 1, no. 7, and no. 8) and restored the expression of *Cyba* by transducing a retrovirus expressing *Cyba* in which the codon usage at the complementary region of sgRNA was altered so that the transduced *Cyba* cDNA is not mutagenized by CRISPR/Cas9. After confirming the restoration of p22<sup>phox</sup> expression by Western blotting (Fig. 6E), we examined ROS production at 4 h after BCR ligation. ROS production at this time point was restored in all the clones in which *Cyba* expression was restored (Fig. 6F, 6G). Thus, the loss of prolonged ROS production in *Cyba*<sup>-/-</sup> BAL17 cells is a consequence of the loss of *Cyba* but not off-target effects of CRISPR/Cas9.

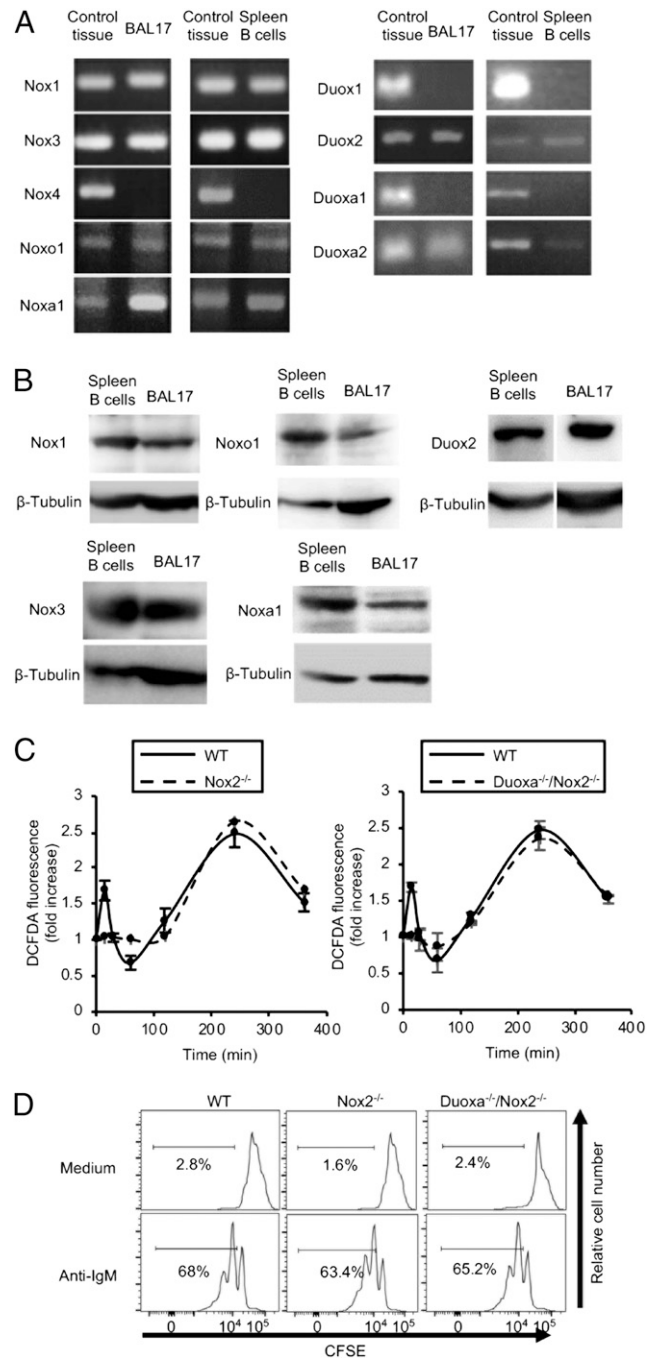


**FIGURE 5.** DUOX1, DUOX2, and NOX2 are dispensable for BCR ligation-induced ROS production in the late phase and B cell proliferation. (A and B) RT-PCR assay (A) and Western blotting (B) for the expression of various NOX isoforms and their regulators in spleen B cells and BAL17 cells. The following tissues were used as control tissues in RT-PCR assay: colon for NOX1, NOXO1, and NOXA1; testis for NOX3; kidney for NOX4; and thyroid gland for DUOX1, DUOX2, DUOX1A1, and DUOX2A2. (C and D) Either CFSE-labeled (D) or unlabeled (C) spleen B cells from wild-type (WT), *NOX2*<sup>-/-</sup> and *NOX2*<sup>-/-</sup> *DUOX1*<sup>-/-</sup> mice were stimulated with 10 μg/ml anti-IgM Ab for the indicated times (C) or 72 h (D). Fluorescence of DCFDA (C) or CFSE (D) were measured by flow cytometry. Fold changes in mean fluorescence intensity of DCFDA fluorescence compared with untreated cells were calculated (C). Alternatively, percentages of proliferated cells are indicated (D).

To address the role of *Cyba* in B cell development, we generated *Cyba*<sup>-/-</sup> mice by CRISPR-mediated genome editing using cloning-free CRISPR/Cas system (45), including crRNAs for



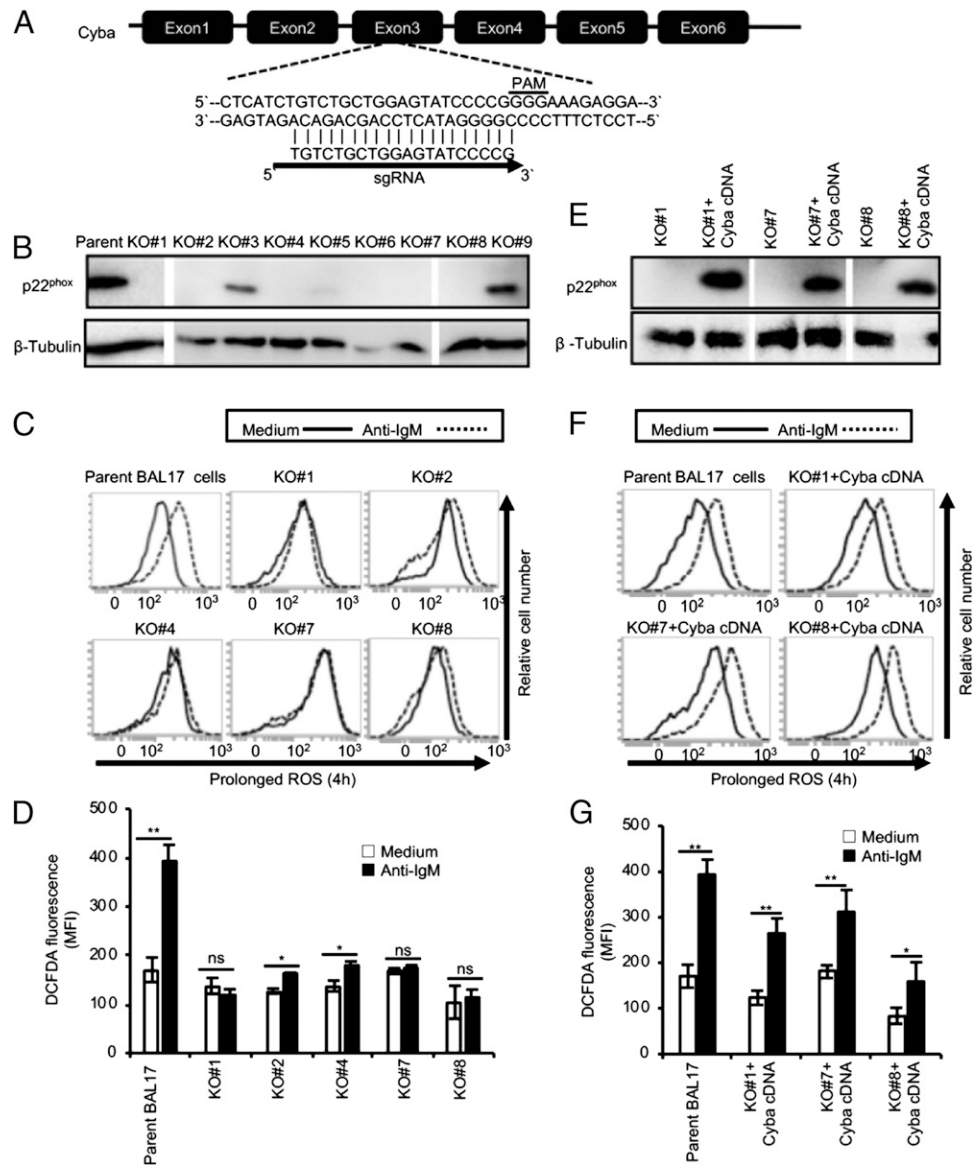


**FIGURE 6.** CRISPR/Cas9-mediated deletion of the *Cyba* gene coding for the NOX regulator p22<sup>phox</sup> abrogates BCR ligation-induced prolonged ROS production in BAL17 cells. **(A)** Schematic representation of sgRNA-targeting exon 3 of the *Cyba* gene. **(B)** Generation of *Cyba*<sup>-/-</sup> BAL17 cells using the lentivirus vector lentiCRISPR containing sgRNA shown in (A). *Cyba*-targeted cells were enriched by puromycin selection. Western blot analysis for p22<sup>phox</sup> in puromycin-resistant clones is shown. **(C and D)** Indicated *Cyba*<sup>-/-</sup> BAL17 clones were stimulated with anti-IgM for 4 h. Cells were loaded with DCFDA, and DCFDA fluorescence was measured by flow cytometry (C). Fold changes in mean fluorescence intensity (MFI) of DCFDA fluorescence compared with untreated cells were calculated. Mean  $\pm$  SD of triplicate is shown (D). \**p* < 0.05, \*\**p* < 0.01; ns, not significant (Student *t* test). **(E)** Restoration of p22<sup>phox</sup> expression in indicated *Cyba*<sup>-/-</sup> BAL17 clones by retrovirus transduction of the *Cyba* cDNA. After the sorting of RFP<sup>+</sup> cells, cells were analyzed by Western blotting for p22<sup>phox</sup> expression. **(F and G)** *Cyba*-restored *Cyba*<sup>-/-</sup> BAL17 cells were stimulated with anti-IgM for 4 h. Cells were loaded with DCFDA, and DCFDA fluorescence was measured by flow cytometry (F). Fold changes in MFI of DCFDA fluorescence compared with untreated cells were calculated. Mean  $\pm$  SD of triplicate is shown (G). \**p* < 0.05, \*\**p* < 0.01 (Student *t* test).

*Cyba* (Supplemental Fig. 2A). We obtained five independent mouse lines and confirmed the lack of p22<sup>phox</sup> expression in all these five lines by Western blot (Supplemental Fig. 2B). Analysis of bone marrow, spleen, and peritoneal cells showed that development of pro-B/pre-B cells and immature and transitional B cells in bone marrow; transitional B cells, follicular B cells, and marginal zone B cells in spleen; and B-1a and B-1b cells in peritoneal cells in *Cyba*<sup>-/-</sup> mice are comparable to those in wild-type mice (Supplemental Fig. 2C–E). This result indicates that *Cyba* does not regulate B cell development and suggests that tonic BCR signaling does not involve *Cyba*-mediated ROS production.

Among the NOXes regulated by p22<sup>phox</sup>, NOX4 is not expressed in B cells, and NOX2 deficiency does not cause reduction in ROS

production, suggesting that NOX1, NOX3, or both are involved in BCR ligation-induced prolonged ROS production. To address the role of NOX1 and NOX3, we deleted these genes by a CRISPR/Cas9 system in BAL17 cells (Fig. 7A, 7B). After confirming the deletion of NOX1 and NOX3 in three independent clones, each by Western blotting (Fig. 7C, 7D), we stimulated *NOX1*<sup>-/-</sup> and *NOX3*<sup>-/-</sup> BAL17 cells with anti-IgM. *NOX1*<sup>-/-</sup> clones showed prolonged ROS production comparable to that in parent BAL17 cells (Fig. 7E, 7G). In contrast, prolonged ROS production was markedly reduced or undetectable in *NOX3*<sup>-/-</sup> clones (Fig. 7F, 7H). The basal ROS level in unstimulated *NOX3*<sup>-/-</sup> clones were also reduced compared with that in parent BAL17 cells. These results suggest that NOX3 but not NOX1

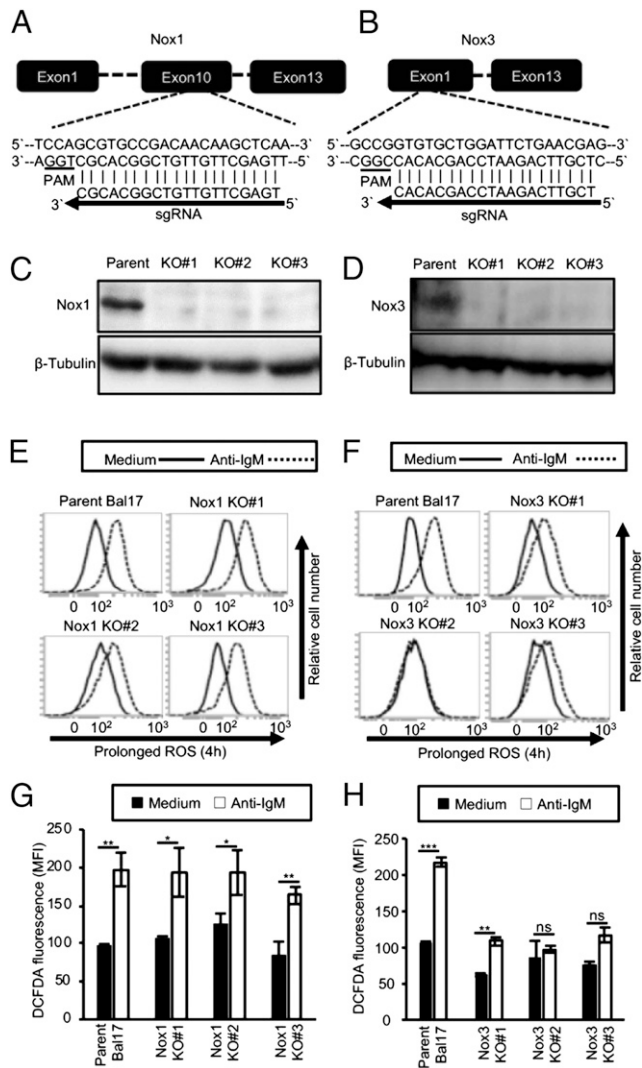


**FIGURE 7.** CRISPR/Cas9-mediated deletion of *NOX3* but not *NOX1* suppresses BCR ligation-induced prolonged ROS production in BAL17 cells. (A and B) Schematic representation of sgRNA-targeting *NOX1* exon 10 and *NOX3* exon 1. (C and D) Generation of *NOX1*<sup>-/-</sup> (C) and *NOX3*<sup>-/-</sup> (D) BAL17 cells using the lentivirus vector lentiCRISPR containing sgRNA shown in (A) and (B), respectively. Western blot analysis for NOX1 (C) and NOX3 (D) in *NOX1*<sup>-/-</sup> and *NOX3*<sup>-/-</sup> clones, respectively, are shown. (E–H) *NOX1*<sup>-/-</sup> (E and G) and *NOX3*<sup>-/-</sup> (F and H) BAL17 clones were stimulated with anti-IgM for 4 h. Cells were loaded with DCFDA, and DCFDA fluorescence was measured by flow cytometry (E and F). Fold changes in mean fluorescence intensity (MFI) of DCFDA fluorescence compared with untreated cells were calculated. Mean  $\pm$  SD of triplicate is shown (G and H). \* $p < 0.05$ , \*\* $p < 0.01$ , \*\*\* $p < 0.001$ ; ns, not significant (Student *t* test).

plays a crucial role in BCR ligation-induced prolonged ROS production.

#### Prolonged ROS production augments activation of NF- $\kappa$ B and AKT

To address how prolonged ROS production enhances B cell activation, we examined activation of the NF- $\kappa$ B and PI3K pathways because these pathways are regulated by ROS (17, 19, 35) and plays a role in B cell survival and proliferation (48–50). We stimulated BAL17 cells and mouse spleen B cells with anti-IgM Ab in the presence or absence of NAC for various times up to 8 h. NAC reduced phosphorylation of NF- $\kappa$ B p65 and various signaling molecules involved in BCR ligation-induced NF- $\kappa$ B activation,

such as I $\kappa$ B, IKK, and CARD11 at 6 and 8 h after BCR ligation (Fig. 8). We addressed the PI3K pathway by analyzing the phosphorylation of AKT in the presence or absence of NAC in mouse spleen B cells. NAC reduced the phosphorylation of AKT at 4–8 h after BCR ligation (Fig. 8). These results suggest that prolonged ROS production augments prolonged activation of both NF- $\kappa$ B and PI3K pathways.

#### Discussion

In this study, we demonstrate that BCR ligation induces ROS production in two phases in both mouse spleen B cells and BAL17 cells. ROS are produced transiently within 1 h in the early phase. In contrast, ROS production in the late phase is sustained from 2 h to more than 6 h after BCR ligation, and the level of ROS was much higher than that in the early phase. Because scavenging ROS by NAC from 3 h after BCR ligation completely inhibited the proliferation of spleen B cells and reduced cell survival, ROS production in the late phase appears to be crucial in B cell activation. This notion is also supported by the finding in *NOX2*<sup>-/-</sup> spleen B cells. In agreement with the previous finding (32, 35), BCR-ligated *NOX2*<sup>-/-</sup> spleen B cells show ROS-dependent proliferation in the absence of ROS production at the early phase. In contrast, the scavenging of ROS by NAC from 3 h after BCR ligation delays the differentiation of B cells to Ab-secreting cells. Previously, plasma cell differentiation was shown to be inhibited in mice deficient in the CDK inhibitor p18<sup>INK4c</sup> (51), suggesting that cell cycle inhibition enhances plasma cell differentiation. Thus, prolonged ROS production may delay plasma cell differentiation by augmenting the proliferation of activated B cells. BCR ligation-induced ROS production in the early phase is transient, and its magnitude is much less than that in the late phase. As a consequence, ROS produced in the early phase may not be able to effectively regulate B cell activation.

In this study, we demonstrate that BCR ligation-induced ROS production in both the early and the late phase is inhibited by NOX inhibitors in both spleen B cells and BAL17 cells. BCR ligation-induced ROS production is also inhibited by CRISPR/Cas9-mediated deletion of either the *Cyba* gene encoding p22<sup>phox</sup>, a common regulator of NOX1–4 (21, 30), or the *NOX3* gene in BAL17 cells. These results indicate that NOXes are involved in BCR ligation-induced early and prolonged ROS production. In contrast, we demonstrate that *Cyba*<sup>-/-</sup> mice show normal B cell development, suggesting that NOXes are involved in BCR ligation-induced signaling but not tonic signaling. We used three distinct NOX inhibitors (i.e., apocynin, DPI, and VAS2870) to address the role of NOXes in BCR ligation-induced ROS production. These three inhibitors almost completely abolished the ROS production. B cell proliferation was also almost completely blocked by apocynin and VAS2870, although we have not tested DPI. DPI and apocynin are classical NOX inhibitors and are less specific. DPI is a general flavoprotein inhibitor and therefore inhibits endothelial NO synthase, xanthine oxidase, and proteins involved in mitochondrial respiration, whereas apocynin carries an ROS-scavenging activity (46). However, VAS2870 is a selective NOX inhibitor without carrying ROS-scavenging activity (47). Thus, the inhibition of ROS production and B cell proliferation by NOX inhibitors including VAS2870 appears to be mediated by NOX inhibition but not off-target effects. BAL17 cells show ROS production in two phases with a similar time course and magnitude with spleen B cells, suggesting ROS production in BAL17 cells represents that in spleen B cells. Thus, abrogation of prolonged ROS production by CRISPR/Cas9-mediated deletion of either *Cyba* that encodes p22<sup>phox</sup> required for the activation of NOX1–4 (21, 30) or *NOX3* in BAL17 cells and restoration of

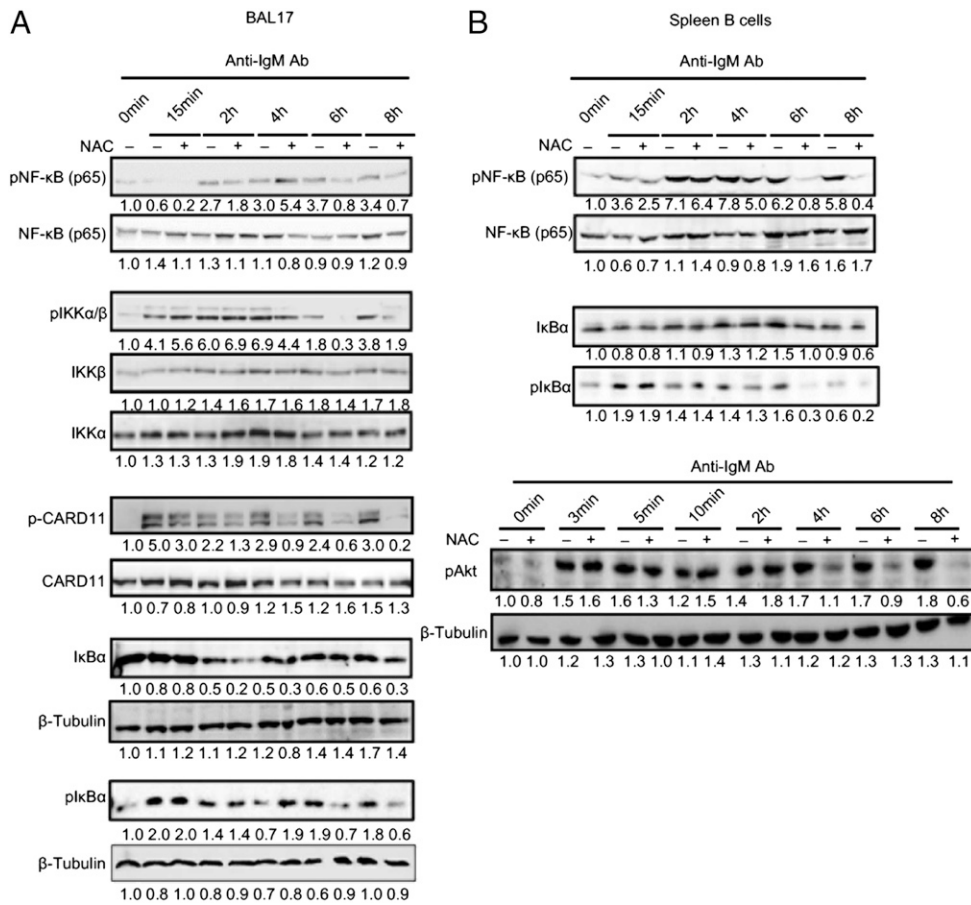


**FIGURE 8.** ROS augment sustained NF-κB activation induced by BCR ligation. BAL17 cells (**A**) and spleen B cells obtained from C57BL/6 mice (**B**) were stimulated with anti-IgM for the indicated times in the presence or absence of NAC. Total cell lysates were analyzed by Western blotting using Abs to the indicated molecules. Band intensities were quantified and expressed as fold-change relative to unstimulated cells (0 min).

prolonged ROS production by expression of *Cyba* in *Cyba*<sup>-/-</sup> BAL17 cells strongly support the notion that BCR ligation-induced prolonged ROS production is mediated by NOXes.

Previously, Wheeler and DeFranco reported that BCR ligation-induced ROS production in the late phase involves mitochondria (35). They detected ROS production in mitochondria using the mitochondria-targeted ROS indicator MitoSOX in the late phase and failed to detect expression of NOXes except for NOX2 by RT-PCR. In this study, we demonstrated that mitochondrial ROS production was not detected in either spleen B cells or BAL17 cells. The cause of the difference between our results and the results by Wheeler and DeFranco is not clear but might be a difference in the culture condition of B cells as mitochondrial ROS production is induced by various stresses. Moreover, we clearly detected the expression of various NOXes, such as NOX1, NOX3, and DUOX2 and their regulators NOXA1, NOXO1, and DUOXA2 by RT-PCR in both BAL17 and spleen B cells. NOXes are expressed highly in specific tissues depending on the NOX isoforms. NOX1, NOX3, NOX4, and DUOX2 are highly expressed in colon, cochlea, kidney, and thyroid gland, respectively (19). However, NOXes are less abundantly expressed in various tissues but play a crucial role in various biological phenomena. For example, mice deficient in NOX1 shows various changes in cardiovascular system (52). Probably because of the low-level expression of various NOXes in B cells, expression of these NOXes were not detected in the study by Wheeler and DeFranco, but this does not exclude the expression of these NOXes or their functional activities in B cells.

In this study, we demonstrate that BCR ligation-induced ROS production in the late phase involves NOX3, whereas NOX2 is responsible for the ROS production in the early phase. Each NOX isoform shows distinct activation mechanisms (21, 30). NOX2 activation requires the recruitment of cytosolic regulators, such as p47<sup>phox</sup>, p67<sup>phox</sup>, and p40<sup>phox</sup>, which is initiated by the phosphorylation of p47<sup>phox</sup>. In contrast, NOX3 activation requires the recruitment of NOXA1 and NOXO1, in which NOXO1 phosphorylation plays a crucial role (53, 54). NOX2 requires Rac1 activation, whereas NOX1 depends less on Rac1 activation. Rac1 is not required for NOX3 activation at least in overexpression system (55, 56). Probably because of distinct requirement for activation in each NOX isoform, BCR ligation initially activates NOX2 and later activates NOX3 without activating NOX1. Future studies on the activation of different NOX isoforms may elucidate the detailed molecular mechanisms for the switch from NOX2 to NOX3 in BCR ligation-induced ROS production.

In this study, we demonstrate that NOX-dependent sustained ROS production is essential for BCR ligation-induced B cell proliferation. We also demonstrate that ROS generated by NOXes augment sustained NF-κB and AKT after BCR ligation (Fig. 8). ROS-dependent sustained activation of the PI3K pathway is consistent with the previous finding (35). Because NF-κB and PI3K pathways regulate lymphocyte proliferation and survival (48–50), enhanced activation of NF-κB and AKT may be involved in ROS-dependent B cell proliferation and survival in BCR-ligated B cells. Thus, BCR ligation induces NOX-dependent sustained ROS production, thereby inducing B cell proliferation and enhancing B cell

survival by augmenting signaling pathways, including the NF- $\kappa$ B and PI3K pathways. Enhanced receptor signaling by NOXes is consistent with the previous findings that ROS generated by NOXes play a role in signal transduction through cytokine receptors, including IL-1 $\alpha$ , TNF- $\beta$ , and platelet-derived growth factor (PDGF) by augmenting the activation of signaling molecules, such as MAPK and NF- $\kappa$ B (27–29). Although ROS produced by cytokines enhance signaling within 30 min, BCR ligation-induced ROS augment activation of NF- $\kappa$ B and AKT at 2–8 and 6 h after BCR ligation, respectively (Fig. 8), probably because of strong and sustained ROS production during this period. The duration of signaling depends on receptors. In dendritic cells, NF- $\kappa$ B activation induced by cytokines such as TNF- $\alpha$  attenuates in 6 h, whereas CD40 ligation-induced NF- $\kappa$ B activation sustains over 24 h (57). Thus, NOXes enhance BCR signaling as well as cytokine signaling, but enhance sustained but not early BCR signaling because of a distinct time course of NOX activation to that in cytokine signaling.

A role of sustained NOX activation in B cell proliferation suggests a crucial role of sustained BCR signaling in B cell activation. In T cells, sustained TCR signaling is required for T cell responses to Ag stimulation through T cell proliferation and IL-2 production (10, 11, 14). Thus, sustained Ag receptor signaling is required for proliferation of both B and T cells. Studies on sustained TCR signaling revealed a distinct requirement of signaling molecules between early and sustained TCR signaling. Kidins220/ankyrin repeat-rich membrane spanning is shown to be required for TCR ligation-induced sustained but not early ERK activation (13, 15), and hnRNP-K is shown to be a target of ERK during late but not early TCR signaling (12). Moreover, endocytosis is shown to be involved in TCR ligation-induced sustained signaling (14). Although signaling events in late BCR signaling and their roles in B cell activation are poorly understood, our results clearly demonstrate that NOXes, especially NOX3, are specifically involved in late BCR signaling and are required for B cell proliferation.

Both B cells and T cells require sustained Ag receptor signaling for activation but appear to use distinct mechanisms for sustained signaling. In B cells, sustained ROS production maintains sustained activation of signaling molecules, including NF- $\kappa$ B and AKT. To further understand the molecular mechanisms for sustained BCR signaling, mechanisms for sustained NOX activation need to be elucidated.

## Acknowledgments

We thank Dr. T. Kitamura (University of Tokyo, Tokyo, Japan) for reagents.

## Disclosures

The authors have no financial conflicts of interest.

## References

- Kurosaki, T., H. Shinohara, and Y. Baba. 2010. B cell signaling and fate decision. *Annu. Rev. Immunol.* 28: 21–55.
- Kurosaki, T., and M. Hikida. 2009. Tyrosine kinases and their substrates in B lymphocytes. *Immunol. Rev.* 228: 132–148.
- Saijo, K., C. Schmedt, I. H. Su, H. Karasuyama, C. A. Lowell, M. Reth, T. Adachi, A. Patke, A. Santana, and A. Tarakhovskiy. 2003. Essential role of Src-family protein tyrosine kinases in NF- $\kappa$ B activation during B cell development. *Nat. Immunol.* 4: 274–279.
- Weber, M., B. Treanor, D. Depoil, H. Shinohara, N. E. Harwood, M. Hikida, T. Kurosaki, and F. D. Batista. 2008. Phospholipase C-gamma2 and Vav cooperate within signaling microclusters to propagate B cell spreading in response to membrane-bound antigen. [Published erratum appears in 2008 *J. Exp. Med.* 205: 1243.] *J. Exp. Med.* 205: 853–868.
- Choi, M. S., R. D. Brines, M. J. Holman, and G. G. Klaus. 1994. Induction of NF-AT in normal B lymphocytes by anti-immunoglobulin or CD40 ligand in conjunction with IL-4. *Immunity* 1: 179–187.
- Reth, M., and T. Brummer. 2004. Feedback regulation of lymphocyte signalling. *Nat. Rev. Immunol.* 4: 269–277.
- Zhang, J., A. K. Somani, and K. A. Siminovich. 2000. Roles of the SHP-1 tyrosine phosphatase in the negative regulation of cell signalling. *Semin. Immunol.* 12: 361–378.
- Xu, Y., K. W. Harder, N. D. Huntington, M. L. Hibbs, and D. M. Tarlinton. 2005. Lyn tyrosine kinase: accentuating the positive and the negative. *Immunity* 22: 9–18.
- Fruman, D. A., and G. Bismuth. 2009. Fine tuning the immune response with PI3K. *Immunol. Rev.* 228: 253–272.
- Rachmilewitz, J., and A. Lanzavecchia. 2002. A temporal and spatial summation model for T-cell activation: signal integration and antigen decoding. *Trends Immunol.* 23: 592–595.
- Huppa, J. B., and M. M. Davis. 2003. T-cell-antigen recognition and the immunological synapse. *Nat. Rev. Immunol.* 3: 973–983.
- Chang, J. W., T. Koike, and M. Iwashima. 2009. hnRNP-K is a nuclear target of TCR-activated ERK and required for T-cell late activation. *Int. Immunol.* 21: 1351–1361.
- Deswal, S., A. Meyer, G. J. Fiala, A. E. Eisenhardt, L. C. Schmitt, M. Salek, T. Brummer, O. Acuto, and W. W. Schamel. 2013. Kidins220/ARMS associates with B-Raf and the TCR, promoting sustained Erk signaling in T cells. *J. Immunol.* 190: 1927–1935.
- Willinger, T., M. Staron, S. M. Ferguson, P. De Camilli, and R. A. Flavell. 2015. Dynamin 2-dependent endocytosis sustains T-cell receptor signaling and drives metabolic reprogramming in T lymphocytes. *Proc. Natl. Acad. Sci. USA* 112: 4423–4428.
- Poltorak, M., I. Meinert, J. C. Stone, B. Schraven, and L. Simeoni. 2014. Sos1 regulates sustained TCR-mediated Erk activation. *Eur. J. Immunol.* 44: 1535–1540.
- Holmström, K. M., and T. Finkel. 2014. Cellular mechanisms and physiological consequences of redox-dependent signalling. *Nat. Rev. Mol. Cell Biol.* 15: 411–421.
- Schieber, M., and N. S. Chandel. 2014. ROS function in redox signaling and oxidative stress. *Curr. Biol.* 24: R453–R462.
- Reczek, C. R., and N. S. Chandel. 2015. ROS-dependent signal transduction. *Curr. Opin. Cell Biol.* 33: 8–13.
- Prieto-Bermejo, R., and A. Hernández-Hernández. 2017. The importance of NADPH oxidases and redox signaling in angiogenesis. *Antioxidants* 6: E32.
- Pao, L. I., K. Badour, K. A. Siminovich, and B. G. Neel. 2007. Nonreceptor protein-tyrosine phosphatases in immune cell signaling. *Annu. Rev. Immunol.* 25: 473–523.
- Nauseef, W. M. 2008. Biological roles for the NOX family NADPH oxidases. *J. Biol. Chem.* 283: 16961–16965.
- Kaminski, M. M., S. W. Sauer, C. D. Klemke, D. Süß, J. G. Okun, P. H. Kramer, and K. Gülow. 2010. Mitochondrial reactive oxygen species control T cell activation by regulating IL-2 and IL-4 expression: mechanism of ciprofloxacin-mediated immunosuppression. *J. Immunol.* 184: 4827–4841.
- Sena, L. A., S. Li, A. Jairaman, M. Prakriya, T. Ezponda, D. A. Hildeman, C. R. Wang, P. T. Schumacker, J. D. Licht, H. Perlman, et al. 2013. Mitochondria are required for antigen-specific T cell activation through reactive oxygen species signaling. *Immunity* 38: 225–236.
- Bulua, A. C., A. Simon, R. Maddipati, M. Pelletier, H. Park, K. Y. Kim, M. N. Sack, D. L. Kastner, and R. M. Siegel. 2011. Mitochondrial reactive oxygen species promote production of proinflammatory cytokines and are elevated in TNFR1-associated periodic syndrome (TRAPS). *J. Exp. Med.* 208: 519–533.
- Tal, M. C., M. Sasai, H. K. Lee, B. Yordy, G. S. Shadel, and A. Iwasaki. 2009. Absence of autophagy results in reactive oxygen species-dependent amplification of RLR signaling. *Proc. Natl. Acad. Sci. USA* 106: 2770–2775.
- Dostert, C., V. Pétrilli, R. Van Bruggen, C. Steele, B. T. Mossman, and J. Tschopp. 2008. Innate immune activation through Nalp3 inflammasome sensing of asbestos and silica. *Science* 320: 674–677.
- Tsutsumi, R., J. Harizanova, R. Stockert, K. Schröder, P. I. H. Bastiaens, and B. G. Neel. 2017. Assay to visualize specific protein oxidation reveals spatiotemporal regulation of SHP2. *Nat. Commun.* 8: 466.
- Li, Q., N. Y. Spencer, F. D. Oakley, G. R. Buettner, and J. F. Engelhardt. 2009. Endosomal Nox2 facilitates redox-dependent induction of NF- $\kappa$ B by TNF- $\alpha$ . *Antioxid. Redox Signal.* 11: 1249–1263.
- Li, Q., M. M. Harraz, W. Zhou, L. N. Zhang, W. Ding, Y. Zhang, T. Eggleston, C. Yeaman, B. Banfi, and J. F. Engelhardt. 2006. Nox2 and Rac1 regulate H2O2-dependent recruitment of TRAF6 to endosomal interleukin-1 receptor complexes. *Mol. Cell Biol.* 26: 140–154.
- Brandes, R. P., N. Weissmann, and K. Schröder. 2014. Nox family NADPH oxidases: molecular mechanisms of activation. *Free Radic. Biol. Med.* 76: 208–226.
- Wienands, J., O. Larbolette, and M. Reth. 1996. Evidence for a preformed transducer complex organized by the B cell antigen receptor. *Proc. Natl. Acad. Sci. USA* 93: 7865–7870.
- Richards, S. M., and E. A. Clark. 2009. BCR-induced superoxide negatively regulates B-cell proliferation and T-cell-independent type 2 Ab responses. *Eur. J. Immunol.* 39: 3395–3403.
- Singh, D. K., D. Kumar, Z. Siddiqui, S. K. Basu, V. Kumar, and K. V. Rao. 2005. The strength of receptor signaling is centrally controlled through a cooperative loop between Ca<sup>2+</sup> and an oxidant signal. *Cell* 121: 281–293.
- Capasso, M., M. K. Bhamrah, T. Henley, R. S. Boyd, C. Langlais, K. Cain, D. Dinsdale, K. Pulford, M. Khan, B. Musset, S. Shadel, et al. 2010. HVCN1 modulates BCR signal strength via regulation of BCR-dependent generation of reactive oxygen species. *Nat. Immunol.* 11: 265–272.
- Wheeler, M. L., and A. L. DeFranco. 2012. Prolonged production of reactive oxygen species in response to B cell receptor stimulation promotes B cell activation and proliferation. *J. Immunol.* 189: 4405–4416.
- Pollock, J. D., D. A. Williams, M. A. Gifford, L. L. Li, X. Du, J. Fisherman, S. H. Orkin, C. M. Doerschuk, and M. C. Dinuer. 1995. Mouse model of X-linked chronic granulomatous disease, an inherited defect in phagocyte superoxide production. *Nat. Genet.* 9: 202–209.

37. Grasberger, H., X. De Deken, O. B. Mayo, H. Raad, M. Weiss, X. H. Liao, and S. Refetoff. 2012. Mice deficient in dual oxidase maturation factors are severely hypothyroid. *Mol. Endocrinol.* 26: 481–492.
38. Nomura, T., H. Han, M. C. Howard, H. Yagita, H. Yakura, T. Honjo, and T. Tsubata. 1996. Antigen receptor-mediated B cell death is blocked by signaling via CD72 or treatment with dextran sulfate and is defective in autoimmunity-prone mice. *Int. Immunol.* 8: 867–875.
39. Oka, Y., A. G. Rolink, J. Andersson, M. Kamanaka, J. Uchida, T. Yasui, T. Kishimoto, H. Kikutani, and F. Melchers. 1996. Profound reduction of mature B cell numbers, reactivities and serum Ig levels in mice which simultaneously carry the XID and CD40 deficiency genes. *Int. Immunol.* 8: 1675–1685.
40. Kitamura, T., Y. Koshino, F. Shibata, T. Oki, H. Nakajima, T. Nosaka, and H. Kumagai. 2003. Retrovirus-mediated gene transfer and expression cloning: powerful tools in functional genomics. *Exp. Hematol.* 31: 1007–1014.
41. Sanjana, N. E., O. Shalem, and F. Zhang. 2014. Improved vectors and genome-wide libraries for CRISPR screening. *Nat. Methods* 11: 783–784.
42. Shalem, O., N. E. Sanjana, E. Hartenian, X. Shi, D. A. Scott, T. Mikkelsen, D. Heckl, B. L. Ebert, D. E. Root, J. G. Doench, and F. Zhang. 2014. Genome-scale CRISPR-Cas9 knockout screening in human cells. *Science* 343: 84–87.
43. Liu, J., E. Xiong, H. Zhu, H. Mori, S. Yasuda, K. Kinoshita, T. Tsubata, and J. Y. Wang. 2017. Efficient induction of Ig gene hypermutation in ex vivo-activated primary B cells. *J. Immunol.* 199: 3023–3030.
44. Onishi, M., S. Kinoshita, Y. Morikawa, A. Shibuya, J. Phillips, L. L. Lanier, D. M. Gorman, G. P. Nolan, A. Miyajima, and T. Kitamura. 1996. Applications of retrovirus-mediated expression cloning. *Exp. Hematol.* 24: 324–329.
45. Aida, T., K. Chiyo, T. Usami, H. Ishikubo, R. Imahashi, Y. Wada, K. F. Tanaka, T. Sakuma, T. Yamamoto, and K. Tanaka. 2015. Cloning-free CRISPR/Cas system facilitates functional cassette knock-in in mice. *Genome Biol.* 16: 87.
46. Altenhöfer, S., K. A. Radermacher, P. W. Kleikers, K. Wingler, and H. H. Schmidt. 2015. Evolution of NADPH oxidase inhibitors: selectivity and mechanisms for target engagement. *Antioxid. Redox Signal.* 23: 406–427.
47. ten Freyhaus, H., M. Huntgeburth, K. Wingler, J. Schnitker, A. T. Bäumer, M. Vantler, M. M. Bekhite, M. Wartenberg, H. Sauer, and S. Rosenkranz. 2006. Novel Nox inhibitor VAS2870 attenuates PDGF-dependent smooth muscle cell chemotaxis, but not proliferation. *Cardiovasc. Res.* 71: 331–341.
48. Thome, M. 2004. CARMA1, BCL-10 and MALT1 in lymphocyte development and activation. *Nat. Rev. Immunol.* 4: 348–359.
49. Suzuki, H., S. Matsuda, Y. Terauchi, M. Fujiwara, T. Ohteki, T. Asano, T. W. Behrens, T. Kouro, K. Takatsu, T. Kadowaki, and S. Koyasu. 2003. PI3K and Btk differentially regulate B cell antigen receptor-mediated signal transduction. *Nat. Immunol.* 4: 280–286.
50. Tian, M. T., G. Gonzalez, B. Scheer, and A. L. DeFranco. 2005. Bcl10 can promote survival of antigen-stimulated B lymphocytes. *Blood* 106: 2105–2112.
51. Tourigny, M. R., J. Ursini-Siegel, H. Lee, K. M. Toellner, A. F. Cunningham, D. S. Franklin, S. Ely, M. Chen, X. F. Qin, Y. Xiong, et al. 2002. CDK inhibitor p18(INK4c) is required for the generation of functional plasma cells. *Immunity* 17: 179–189.
52. Gimenez, M., B. M. Schickling, L. R. Lopes, and F. J. Miller, Jr. 2016. Nox1 in cardiovascular diseases: regulation and pathophysiology. *Clin. Sci. (Lond.)* 130: 151–165.
53. Yamamoto, A., R. Takeya, M. Matsumoto, K. I. Nakayama, and H. Sumimoto. 2013. Phosphorylation of Nox1 at threonine 341 regulates its interaction with Noxa1 and the superoxide-producing activity of Nox1. *FEBS J.* 280: 5145–5159.
54. Debbabi, M., Y. Kroviarski, O. Bournier, M. A. Gougerot-Pocidallo, J. El-Benna, and P. M. Dang. 2013. NOXO1 phosphorylation on serine 154 is critical for optimal NADPH oxidase 1 assembly and activation. *FASEB J.* 27: 1733–1748.
55. Miyano, K., N. Ueno, R. Takeya, and H. Sumimoto. 2006. Direct involvement of the small GTPase Rac in activation of the superoxide-producing NADPH oxidase Nox1. *J. Biol. Chem.* 281: 21857–21868.
56. Ueno, N., R. Takeya, K. Miyano, H. Kikuchi, and H. Sumimoto. 2005. The NADPH oxidase Nox3 constitutively produces superoxide in a p22phox-dependent manner: its regulation by oxidase organizers and activators. *J. Biol. Chem.* 280: 23328–23339.
57. O'Sullivan, B. J., and R. Thomas. 2002. CD40 ligation conditions dendritic cell antigen-presenting function through sustained activation of NF-kappaB. *J. Immunol.* 168: 5491–5498.